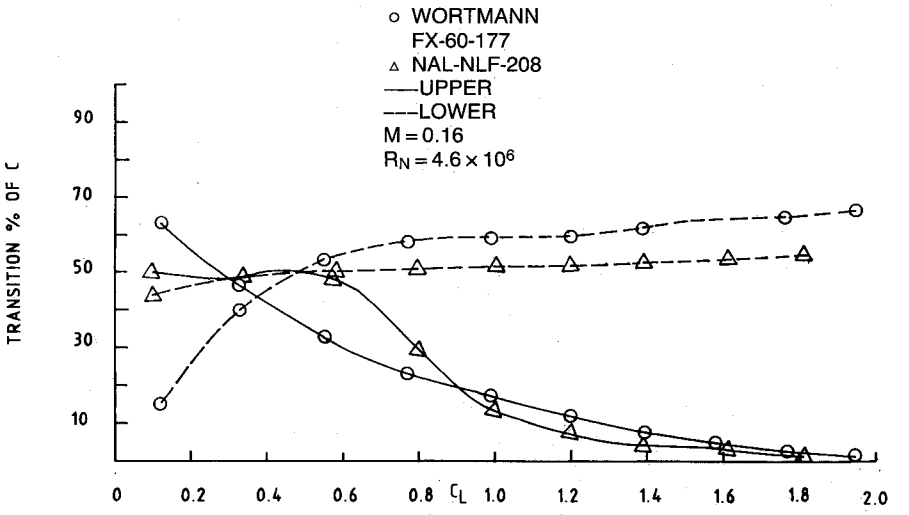

Fig. 4 Transition of the NAL-NLF-208 and FX-60-177 airfoils.

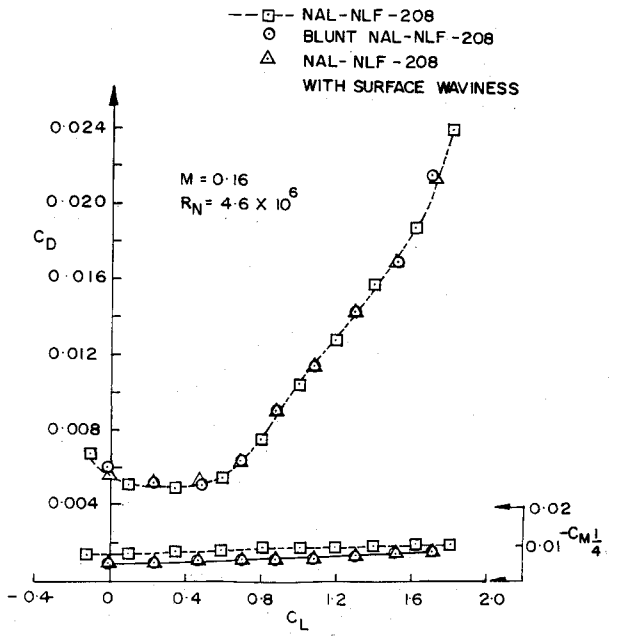

Fig. 5 Drag polars for the NAL-NLF-208 and the modified NAL-NLF-208.

NAL-NLF-208. As can be seen in Fig. 5, this waviness had no significant effect on the NAL-NLF-208 airfoil.

Conclusion

The analysis presented points out that the NAL-NLF-208 airfoil (with bluntness) is robust in performance and is practically feasible. Wind-tunnel and flight testing of this airfoil are worth pursuing.

Acknowledgment

The authors are grateful to R. Narasimha, Director of NAL, for critically reviewing this Note and making a number of valuable suggestions toward its improvement.

References

[1]Ramamoorthy, P., "A New Method for Designing Natural Laminar Flow Airfoils," National Aeronautical Laboratory, Bangalore, India, Rept. NAL PD-FM-8821, Dec. 1988.

[2]Ramamoorthy, P., and Ramesh, S., "Design of a Natural Laminar Flow Airfoil (NAL-NLF-170) for General Aviation Application," National Aeronautical Laboratory, Bangalore, India, Rept. NAL PD-FM-8820, Dec. 1980.

[3]Goldstein, S., "Low Drag and Suction Airfoil," *Journal of the Aeronautical Sciences*, Vol. 15, April 1948, pp. 189–220.

[4]Abbott, I. H., and Von Doenhoff, A. E., *Theory of Wing Sections*, Dover, New York, 1959, pp. 73–75.

[5]Ramamoorthy, P., and Dhanalakshmi, K., "NCSU Code: Validation and Extension on NAL's UNIVAC 1100/60 System," National Aeronautical Laboratory, Bangalore, India, Rept. NAL PD-FM-8716, May 1987.

[6]Althaus, D., "Experimental Results from Laminar Wind Tunnel of the Institute for Aerodynamics and Gasdynamics, University of Stuttgart 1962–1972," Departmental publication, Univ. of Stuttgart, Germany.

[7]Stevens, W. A., et al., "Mathematical Model for Two-Dimensional Multicomponent Airfoils in Viscous Flow," NASA CR-1843, July 1971.

Measurements and Implications of Vortex Motions Using Two Flow-Visualization Techniques

Donald P. Delisi*
Northwest Research Associates, Inc., Bellevue, Washington 98005
and
George C. Greene†
NASA Langley Research Center, Hampton, Virginia 23665

Introduction

VORTEX flows represent a challenge in aircraft design because they occur at many different scales and are important for almost every aspect of vehicle performance, stability, control, and maneuverability. This is especially true for highly maneuverable fighter aircraft, which may have extensive regions of complex, turbulent, off-surface vortex flow for which there are no reliable computational design methods. In

Received April 2, 1990; accepted for publication April 9, 1990.

*Senior Research Scientist. Member AIAA.

†Research Engineer, Fluid Mechanics Division. Associate Fellow AIAA.

addition, aircraft wake vortices impose limits on aircraft separation during takeoff and landing. Therefore, understanding the migration and decay of aircraft wake vortices is important for maximizing the capacity of crowded airports. Thus, there is an increasing need for quantitative data for a wide range of vortex flows.

Quantitative vortex measurements are sufficiently difficult to make that flow visualization is still a mainstay, state-of-the-art research tool (see, for example, Ref. 1 and the references cited therein). However, even flow-visualization results can be difficult to interpret quantitatively.

The measurements reported herein were made in the trailing wake of a rectangular wing, which is a relatively simple vortex flow. Previous laboratory measurements of trailing wake vortices from similar wings have suggested maximum limits on the vertical migration and lifetime of vortices in both unstratified and stratified environments.[2] Similar maximum limits for full-scale aircraft wakes have been reported, although meteorological measurements generally were not made to determine the environmental conditions present during the tests.[3]

In this Note, we present laboratory measurements of trailing wake vortices using two different, but complementary, flow-visualization techniques. The two techniques yield different interpretations of vortex migration distance and lifetime. Thus, this Note will focus on the difficulty in determining vortex evolution and lifetime from flow-visualization measurements.

Experimental Facility

The experiments were performed in a water-filled towing tank measuring 9.8 m long, 0.9 m wide, and 1.0 m deep. The water depth was 0.9 m. To generate vortices, we used a rectangular wing that had a circular-arc airfoil shape, modified with a rounded leading edge. The top surface had a radius of 8.3 cm, and the bottom, flat surface was 6.4 cm long before rounding. This resulted in a maximum thickness of 0.64 cm at the half-chord point. Rounding the leading edge of the wing reduced the airfoil chord to 5.8 cm. The wingspan was 9.9 cm (aspect ratio of 1.7), and the wingtips were rounded.[2] The wing was attached to a strut with a chord of 3.8 cm and a thickness of 0.3 cm. The strut itself was attached to a carriage, which rode above the tank and was towed by steel cables. The towing speed for this study was 77 cm/s, yielding a chord Reynolds number of 4.5×10^4. The angle of attack was 13.6 deg.

Fluorescein dye was emitted from both wingtips through small tubes embedded in the wing. Neutrally buoyant particles were also seeded uniformly in the tank.[4,5] The dye and particle motions were observed both with general lighting from the top and side of the tank and with a light slit oriented perpendicular to the path of the wing. The light slit measured 7.3 cm wide and was illuminated by two theatrical spotlights. Observations of vortex motions were made using two 35-mm cameras and a video camcorder. One of the 35-mm cameras was located on the bottom of the tank 1.8 m from the light slit. The other 35-mm camera and the video camcorder were located either at the side or the top of the tank. The 35-mm cameras were used to take time exposures of the particle motions, resulting in streak photographs, and to record the motion of the dye. The video camcorder was used primarily to record the motion of the dye. Time histories of the vortex motions were obtained from both the motion of the dye and the streak photographs.

Laboratory Results

Figure 1 shows vortex migration measurements from our study as well as results from previous studies. In this figure, H is the nondimensional vortex rise height and T the nondimensional time, where

$$H = h/b_0 \qquad \text{and} \qquad T = (V_0 t)/b_0$$

where h is the vortex height at time t, b_0 the initial vortex separation, V_0 the initial vortex migration rate, and t the dimensional time. Here, $h = 0$ at $t = 0$. The dashed line is $H = T$ and represents the time history for inviscid point vortices. It is well known, however, that real vortices initially rise on the inviscid line but deviate from it at later times.[2,6]

In Fig. 1, the circles represent our laboratory results for dyed wake measurements. The crosses in Fig. 1 represent laboratory towing-tank results from Sarpkaya,[2] who towed three-dimensional wings similar to those used in the present study. The results shown are Sarpkaya's detailed dye measurements in an unstratified flow. The plus symbols in Fig. 1 are vortex measurements from Tomassian,[6] who generated two-dimensional vortices with a plunger in an unstratified water tank and used dye to visualize the vortices. Note four important points: 1) the results shown were all obtained by using dye to visualize the motion of the vortices, 2) the results from all investigators are reasonably consistent, 3) the measurements all end at roughly the same value of T, and 4) the vortices all rise to approximately the same value of H when the measurements end.

Figure 2 shows our results for vortex measurements using particle streaks. Here, the squares are our particle streak results, the dashed line is $H = T$, and the stippled region shows the range of dye measurements from Fig. 1. Note that the particle streak measurements in Fig. 2 extend to a much larger value of T and that the vortices migrate to a much larger value of H than shown in Fig. 1. Yet, the particle streak measure-

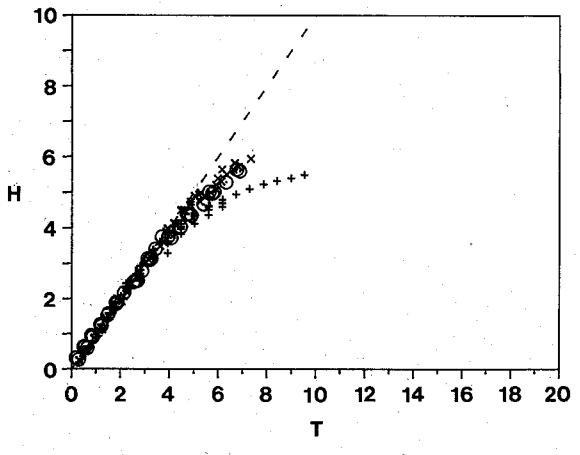

Fig. 1 H vs T for laboratory vortex measurements in unstratified flows using dye for flow visualization. Crosses are from Ref. 2, and plus symbols are from Ref. 6. The circles are our dyed wake laboratory measurements. The dashed line is $H = T$.

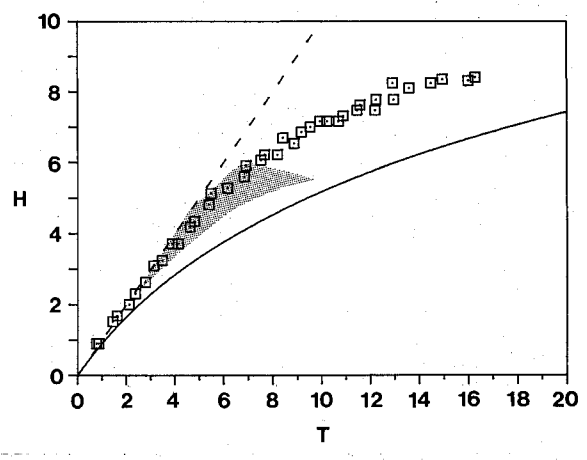

Fig. 2 H vs T for laboratory vortex measurements in unstratified flows. Squares are our particle streak measurements. The stippled region encompasses the range of dye measurements from Fig. 1. The dashed line is $H = T$. The solid line is a prediction from Greene.[7]

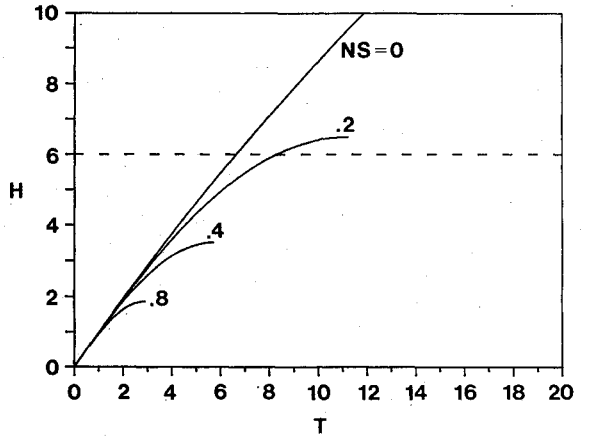

Fig. 3 Predictions from Greene[7] of the effect of density stratification on wake vortex motion for a Boeing 747 with $NS = 0$. The dashed line is $H = 6$.

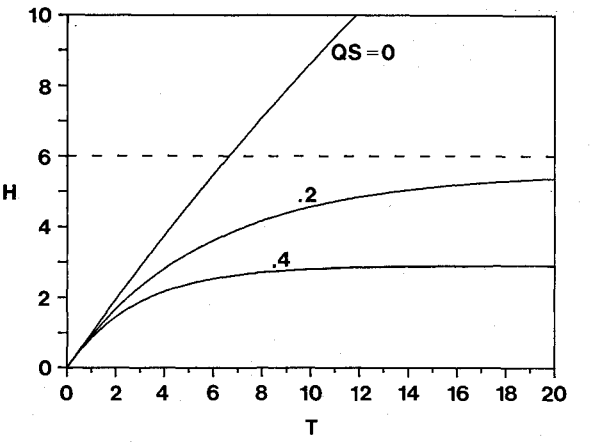

Fig. 4 Predictions from Greene[7] of the effect of ambient turbulence on wake vortex motion for a Boeing 747 with $QS = 0$. The dashed line is $H = 6$.

ments agree at early times with the dye measurements. The difference between dye and particles in our observations is because dye disperses due to vortex breakdown and dissipation. When this occurs, there are either very weak concentrations of dye left in the flow, and the region of vortex motion disappears, or, if sufficient dye is remaining, the center of the vortex flow no longer can be determined. The particles, however, do not lose concentration like dye, and it is possible to follow the particle motions long after the passive tracer has dissipated.

Two obvious questions arise at this point: Is there a difference in the flowfield when one uses dye vs particles for flow visualization? Why did previous investigators not observe longer vortex lifetimes? We believe the answers to these two questions are interrelated. To answer these questions, we performed experiments using both dye and particles simultaneously. Those experiments showed that dye and particles give the same vortex centers for early times, as implied by Figs. 1 and 2. Thus, the choice of flow-visualization method does not alter the flowfield. When the vortex cores burst, however, dye concentrations become more uniform, and vortical motions become difficult to discern since gradients in dye concentrations are small. Particle motions outside the core, however, do not change significantly as the dye disperses, and vortical motions using particle streaks are clearly visible to the very end of our measurements. In previous investigations, the vortex cores probably also burst, and dye concentrations became weaker and more uniform. The subsequent difficulty in seeing vortical motions in the resulting dye field probably gave the false impression that the vortices had decayed and died. Using particles instead of dye for flow visualization shows that the vortices do not die when the cores burst but continue to migrate long after the dye disperses.

It is important to note that the particle streak results shown in Fig. 2 do not indicate the maximum rise heights or the maximum lifetimes of our laboratory vortices. Rather, the measurements in Fig. 2 were terminated not because the vortices ceased to exist or ceased to be discernible from the background, but because the vortices were in ground effect with the bottom of the tank. (In fact, the vortices in Fig. 2, on reaching the bottom of the tank, migrated horizontally along the bottom and started moving up the sidewalls of the tank before eventually dissipating.) Thus, the results in Fig. 2 are facility-limited, and the ultimate lifetime and migration distance of vortices in a quiescent laboratory environment are still, in the authors' opinion, open questions. The solid line in Fig. 2 is from Greene,[7] using the parameters of our experiments. Note that, although the fit is not exact, the model result of Ref. 7 approximates the trend of the particle data.

Full-Scale Predictions

Based on the success of Greene's model in predicting the greater migration distances and longer lifetimes observed in the current laboratory measurements, full-scale aircraft predictions were made to determine if the wake migration limits observed in flight tests were really upper limits or, rather, were due to prevailing atmospheric conditions. The parameters chosen for investigation were atmospheric turbulence and density stratification, caused by a nonadiabatic temperature lapse rate.

The maximum, measured vortex migration for full-scale aircraft is about 900 ft, based primarily on observations of Boeing 747 wakes at altitude.[3] For the B-747, the initial vortex spacing is about 150 ft (plus or minus about 10 ft), and the wake requires about 20 s to descend that distance in the landing configuration and about 35 s in the cruise configuration.[3] Therefore, the maximum vortex migration corresponds to a nondimensional distance H of about 6, and each nondimensional time unit corresponds to about 20 or 35 s, depending on the configuration.

Figure 3 shows the predicted, nondimensional vortex migration characteristics using Greene's model as a function of the density stratification parameter NS for conditions with no atmospheric turbulence. Here $NS = (Nb_0)/V_0$ where N is the Brunt-Vaisala frequency defined by

$$N = \left[-\frac{g}{\rho}\frac{d\rho}{dz} - \frac{g^2}{c^2} \right]^{1/2}$$

where ρ is density, g the acceleration due to gravity, z the vertical coordinate, and c the speed of sound.

The 900-ft descent limit is indicated by the dashed line corresponding to $H = 6$. For the B-747, $NS = 0$ is the unstratified case, corresponding to an adiabatic lapse rate in the atmosphere. For a slightly stable "standard" atmosphere, NS is about 0.2 for the landing configuration and about 0.4 for the cruise configuration. It is important to note that only a 1°C/100 m change in lapse rate is required to change NS from 0.4 to 0.2 for the landing configuration, which doubles the predicted wake lifetime. Larger values of NS correspond to strongly stratified conditions and shorter wake lifetimes. For example, $NS = 0.8$ corresponds to an inversion (4°C/100 m) for the landing configuration.

The atmosphere is rarely completely free of turbulence, and even small amounts may significantly accelerate wake decay. Figure 4 shows the predicted effects of turbulence on vortex migration in an unstratified atmosphere. For the B-747 landing configuration, a turbulence parameter QS of 0.2 corresponds roughly to the upper boundary of what is termed

"negligible" turbulence for this aircraft. Here $QS = q/V_0$, where q is the root-mean-square (rms) turbulence velocity. The QS value for a given level of turbulence is almost twice as large for the cruise configuration as for the landing configuration.

Thus, from the model results shown in Figs. 3 and 4 for a B-747 aircraft, even small amounts of density stratification or atmospheric turbulence could cause the observation of an $H = 6$ limit on wake migration, and this is especially true for the cruise configuration. It is not known how often the conditions of near-zero stratification and turbulence occur. However, they may occur so infrequently that they do not normally affect aircraft operations.

Concluding Remarks

The data in Figs. 1 and 2 indicate that the choice of flow-visualization method used in an experiment can have an important influence on the interpretation of the maximum vortex lifetime and the maximum vortex migration distance. Vortices are observed to migrate farther and last longer using neutrally buoyant particles rather than using dye to visualize the vortex motion. Similarly, Figs. 3 and 4 show that the maximum, measured full-scale vortex descent distance may be influenced strongly by atmospheric conditions (which were not measured during most flight tests). Thus, the 900-ft descent distance, which is commonly thought to be the maximum migration limit for full-scale aircraft, may not, in fact, be the maximum limit.

The new, laboratory wake measurements presented here are significant in their own right; however, the authors believe these results and the implications of incorporating different visualization techniques may be of interest to researchers studying other aircraft vortex flows.

The evolution and migration of vortices is applicable to a wide class of aerospace problems. The data presented here point out the deficiencies in our current understanding of vortex motions. The evolution is even less well understood if we include ground effect, wind, and other environmental factors.

Acknowledgments

This study was supported by the Office of Naval Research under Contracts N00014-88-C-0284 and N00014-89-C-0030. The authors thank Lee E. Piper and Raminder Singh for useful discussions and their assistance in performing the experiments. Thanks also to T. Sarpkaya for useful discussions on an early draft of this Note.

References

[1]Campbell, J. F., Chambers, J. R., and Rumsey, C. L., "Observation of Airplane Flowfields by Natural Condensation Effects," *Journal of Aircraft,* Vol. 26, July 1989, pp. 593–604.

[2]Sarpkaya, T., "Trailing Vortices in Homogeneous and Density-Stratified Media," *Journal of Fluid Mechanics,* Vol. 136, Nov. 1983, pp. 85–109.

[3]Condit, P. M., and Tracy, P. W., "Results of the Boeing Company Wake Turbulence Test Program," *Aircraft Wake Turbulence and Its Detection,* edited by J. H. Olsen, A. Goldburg, and M. Rogers, Plenum, New York, 1971, pp. 473–508.

[4]Delisi, D. P., and Orlanski, I., "On the Role of Density Jumps in the Reflexion and Breaking of Internal Gravity Waves," *Journal of Fluid Mechanics,* Vol. 69, Pt. 3, 1975, pp. 445–464.

[5]Delisi, D. P., and Dunkerton, T. J., "Laboratory Observations of Gravity Wave Critical-Layer Flows," *Pure and Applied Geophysics,* Vol. 130, No. 2/3, 1989, pp. 445–461.

[6]Tomassian, J. D., "The Motion of a Vortex Pair in a Stratified Medium," Ph.D. Thesis, Univ. of California, Los Angeles, CA, 1979.

[7]Greene, G. C., "An Approximate Model of Vortex Decay in the Atmosphere," *Journal of Aircraft,* Vol. 23, July 1986, pp. 566–573.

Airfoil Design for Endurance Unmanned Air Vehicles

Richard M. Howard*
Naval Postgraduate School, Monterey, California 93943

Nomenclature

C_d = airfoil section drag coefficient
C_D = aircraft drag coefficient
C_l = airfoil section lift coefficient
C_L = aircraft lift coefficient
x = streamwise coordinate
y = transverse coordinate
α = angle of attack

Introduction

THE current classifications for unmanned air vehicles (UAVs) for military use include, among others, an endurance UAV with a mission requirement of remaining aloft for a period of days. Though many of the proposed vehicles are large (the Boeing Condor, which set two altitude records in 1989, has a 200-ft wingspan[1]), the high altitudes at which these aircraft are expected to fly place the operating flight conditions in the low Reynolds number regime. In the 1970s, when few general-aviation aircraft manufacturers were designing their own airfoils, it was not uncommon for a manufacturer to select an airfoil from the text of Abbott and von Doenhoff.[2] Sailplane competition had long before driven soaring enthusiasts to consider more highly optimized contours for low Reynolds number flight, resulting in the development of many excellent airfoils by Wortmann and Eppler. It can be expected that many advances in aerodynamics for endurance UAVs will be derived from current sailplane technology.

High-altitude long-endurance propeller-driven unmanned aircraft require not only a high C_L/C_D, but, more importantly for concerns of maximum time aloft, a high value of $C_L^{3/2}/C_D$. This dependence can be noted from the Breguet endurance equation,[3] from which it can also be noted that consideration must be given to the speeds where propeller efficiency and fuel consumption are optimal. Maximizing endurance will in actuality involve a compromise between these various factors. In any case, a high value of the endurance parameter $C_L^{3/2}/C_D$ is certainly desirable. The effect is to weight the high-lift, low-drag benefits toward the high-lift end of the flight spectrum. As noted in Ref. 4, it is not necessarily the airfoil with the lowest drag coefficient that may be optimum; a higher maximum lift coefficient allows the aircraft to have less wing area for a specified minimum airspeed, which reduces the overall wing profile drag. A tradeoff of drag for lift may prove to be worthwhile for a vehicle such as the endurance UAV, which may have very narrow design constraints. A somewhat similar approach was taken for the Voyager aircraft that circled the world without refueling—to avoid the possible loss of lift on the canard from surface contamination, drag-producing vortex generators were attached to the canard's upper surface.

The Eppler method, described in Ref. 5, was used to develop a low Reynolds number airfoil suitable for the requirements of an endurance UAV. Airfoil performance parameters

Received Dec. 1, 1989; revision received March 1, 1990; accepted for publication March 27, 1990.

*Assistant Professor, Department of Aeronautics and Astronautics. Member AIAA.